Research Article

Xin Ai#, Shuqing Lu#, Ailing Xie, Haoran Zhang, Juntao Zhao, Tianjiao Wang, Guoqiang Chen, Shenzhou Lu*, and Tieling Xing*

Fabrication of flexible conductive silk fibroin/polythiophene membrane and its properties

https://doi.org/10.1515/epoly-2022-0004
received September 11, 2021; accepted October 21, 2021

Abstract: Silk fibroin (SF) film is an insulating material, which can be combined with polythiophene derivatives with electrical conductivity to obtain a flexible conductive material. In this work, poly(3,4-ethylenedioxythiophene) (PEDOT) was used to graft a silk protein film. The hydroxyl radical is formed by activation and oxidation of the silk protein film polymerized with the PEDOT radical formed by oxidation of 3,4-ethylenedioxythiophene to obtain a conductive silk film. The SF/PEDOT film, when tested, showed excellent electrical conductivity with resistance up to 63 $\Omega \cdot cm^{-2}$, good flexibility, mechanical properties, fastness, and biocompatibility.

Keywords: silk fibroin, poly(3,4-ethylenedioxythiophene), grafting, flexible conductive membrane

1 Introduction

Traditional electronic products based on mono crystalline silicon, metals, and metal oxides have high rigidity and low ductility, which cannot meet the deformation requirements of non-solid surface applications (1). Flexible electronic products can maintain good electrical conductivity and sensitivity during complex deformation. By outputting physical or chemical signals, they can realize disease diagnosis and health monitoring (2). They have high application value in electronic materials industry and biomedical field (3), which break through the limitations of traditional electronic products, but prolonged contact with human body will cause discomfort. Natural materials have become the preferred substrate for flexible wearable products to satisfy people's pursuit of comfortable and healthy life. Silk fibroin (SF) is a kind of natural protein polymer made from silkworm cocoons degumming, which has excellent mechanical properties (4), diverse process ability, and biodegradability, and is widely used in surgical sutures, tissue engineering scaffolds (5), artificial skin (6), and cartilage tissue (7). However, SF is an insulating material and needs to be compounded with metals, metal oxides, ionic liquids (8), conductive polymers, or carbon materials to improve the electrical conductivity (9). Among them, coating with metal nanoparticles/nanowires can obtain higher conductivity, but the flexibility and durability of the materials are greatly reduced (10). Conductive polymer materials mainly include polyaniline (11), polypyrrole, and polythiophene (10), which are widely used in the conductive modification of silk fibroin due to their easy processing, excellent flexibility, and low-temperature synthesis route.

Among many conductive polymers, poly(3,4-ethylenedioxythiophene) (PEDOT) has the unique structural characteristics of low redox potential, small band gap width, and more electron donating groups (12). It has excellent stability and high conductivity in oxidation state. The degree of π-electron conjugation of polythiophene increases continuously with oxidation, the small difference in length between adjacent carbon-carbon and nitrogen double bonds, and the conductivity increases to a certain extent. Therefore, PEDOT is considered to be the most stable conductive polymer (13,14). At the same time, PEDOT has the characteristics of lightweight, good

# These authors contributed equally to this work.

*** Corresponding author: Shenzhou Lu,** National Engineering Laboratory for Modern Silk, Department of Textile Engineering, College of Textile and Clothing Engineering, Soochow University, Suzhou 215123, China, e-mail: lushenzhou@suda.edu.cn
*** Corresponding author: Tieling Xing,** National Engineering Laboratory for Modern Silk, Department of Light Chemistry Engineering, College of Textile and Clothing Engineering, Soochow University, Suzhou 215123, China, e-mail: xingtieling@suda.edu.cn
Xin Ai, Shuqing Lu, Ailing Xie, Haoran Zhang, Juntao Zhao, Tianjiao Wang, Guoqiang Chen: National Engineering Laboratory for Modern Silk, Department of Light Chemistry Engineering, College of Textile and Clothing Engineering, Soochow University, Suzhou 215123, China
ORCID: Shenzhou Lu 0000-0003-4188-2057; Tieling Xing 0000-0002-4136-3137

Open Access. © 2022 Xin Ai *et al.*, published by De Gruyter. This work is licensed under the Creative Commons Attribution 4.0 International License.

biocompatibility, large specific surface area, easy surface modification (2), good moisture resistance, and film-forming properties (10). Conductive polymers are compounded with natural biomaterials to obtain flexible conductive materials with good biocompatibility (15), such as conductive films. The current synthesis of conductive composites consists of the addition of thiophene monomers, oxidants (such as $FeCl_3$), and dopant solution (16), or the deposition of PEDOT coating on the substrate surface via thiophene monomer vapor (17). The synthesized PEDOT has high degree of branching, uneven polymerization, weak binding ability with the substrate, poor conductivity, and high hardness, which limits the direct use of PEDOT to make flexible conductive materials (18).

In this work, a flexible conductive film with good stability was fabricated through grafting of EDOT onto the surface of the SF film. The SF film can be activated by H_2SO_4 and form hydroxyl radicals under the oxidation of MnO_2, while EDOT can be oxidized by ammonium per-sulfate to form EDOT free radicals, which undergo free-radical polymerization and PEDOT will be successfully grafted onto the surface of the SF film. The preparation mechanism is shown in Figure 1. Thanks to the good biocompatibility of PEDOT and SF, the prepared SF/PEDOT membrane has good prospect in flexible and conductive biomaterials (19).

2 Experimental methods

2.1 Materials

Silkworm (Bombyx mori) cocoons were provided by Suzhou Siruibao Biotechnology Co., Ltd. (Suzhou, China). 3,4-Ethylenedioxythiophene was purchased from Shanghai Titan Technology Co., Ltd. Ammonium per-sulfate was supplied by Shanghai Lingfeng Chemical Reagent Co., Ltd. Sodium bicarbonate was bought from Jiangsu Qiangsheng functional Chemistry Co., Ltd. Glycerol was purchased from Jiangsu Argon Krypton Xenon Material Technology Co., Ltd. Potassium permanganate was purchased from Sinopharm Chemical Reagent Co., Ltd. Cellulose dialysis membrane (8,000–14,000 Da) was bought from Union Carbide Corporation (Houston, TX, USA). All the chemicals were of analytical reagent grade and were used without further purification.

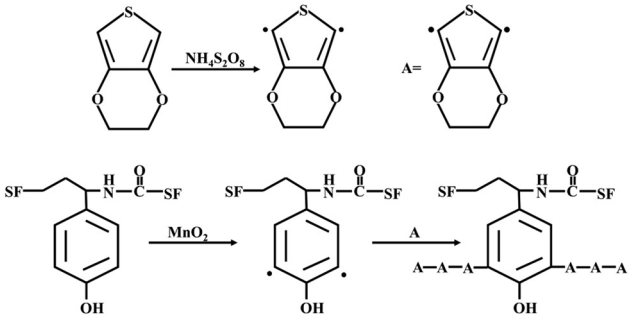

Figure 1: Mechanism of SF/PEDOT membrane preparation.

2.2 Preparation of SF/PEDOT membrane

2.2.1 Preparation of SF solution

Fresh cocoons were added to slightly boiling $NaHCO_3/Na_2CO_3$ buffer solution with pH 9 at a bath ratio of 1:100 for 30 min and then washed with deionized water. The above operation was repeated three times, then the degummed cocoons were dried in an oven at 60°C, and then were dissolved in 9.3 mol·L^{-1} LiBr solution with bath ratio of 15:100 at 65 ± 2°C for 1 h, and cooled. After cooling, the SF solution was obtained by dialysis with cellulose dialysis membrane (8,000–14,000 Da) in deionized water for 3 days.

2.2.2 Preparation of the SF film

The concentration of SF solution was adjusted to 6%, then glycerol was added with the mass ratio of glycerol:SF = 3:10. The mixed solution was cast into the mold at room temperature to obtain the insoluble SF film.

2.2.3 Surface activation of SF film

The insoluble SF film was immersed in 4 mol·L^{-1} H_2SO_4 solution and withdrawn after 4 s of treatment, then immersed in saturated $NaHCO_3$ solution to neutralize for 1 min and washed with deionized water. The activated SF film was immersed in 0.4 mol·L^{-1} potassium permanganate solution at room temperature for 1 min and washed with deionized water to remove the unreacted potassium permanganate.

2.2.4 Preparation of SF/PEDOT membrane

EDOT (0.3 mol·L^{-1}) and ammonium persulfate (0.02 mol·L^{-1}) were added to 100 mL of deionized water, and SF films after

surface activation and oxidation were put into the solution, which were put in the vibration dyeing machine and reacted at 30°C for 30, 60, 120, 240, 480, and 960 min, respectively. After the reaction, the SF film was washed with absolute ethanol and water in turn, then dried at room temperature, and stored at 4–8°C, as shown in Figure 2.

2.3 Characterization of SF/PEDOT membrane

2.3.1 Surface morphology and structural analysis of SF/PEDOT membrane

The surface morphology of SF/PEDOT membrane was observed by using Hitachi S-4800 scanning electron microscope (SEM) under 3 kV accelerating voltage. The energy spectrum analysis was used to detect S and Mn elements in samples. The surface elemental compositions of the samples were measured at a resolution of 3.5 nm (500 V), acceleration voltage of 800 V, and tilt angle of 0° using energy disperse spectroscopy (EDS) analyzer (JEOL JSX-1000S, JEOL, Japan). The surface element content of SF film was analyzed by Thermo Scientific K-Alpha^{+} X-ray photoelectron spectroscopy (Thermo Fisher Scientific Co., Ltd., Waltham, MA, USA) using an Al Ka X-ray source (1486.6 eV). Surface attenuated total reflection Fourier transform infrared (ATR-FTIR) spectra was carried out with Nicolet 5700 instrument. All infrared spectra were recorded in the range of 4,000–550 cm^{-1} using the Nicolet iS5 spectrometer equipped with an iD7 ATR accessory (Thermo Scientific, Waltham, MA, USA). Each spectrum was acquired by the accumulation of 32 scans with a resolution of 4 cm^{-1}. The Raman spectra of SF film were analyzed using a Raman spectrometer (Horiba Jobin, HR800). The measurement range was 200–2,000 cm^{-1}, laser was 638 nm, and filter was 25%.

2.3.2 Mechanical properties

According to ISO37:2005 standard, the SF film was cut into 35 mm × 6 mm dumbbell strips and placed in a room with constant temperature of 20°C and humidity (RH) of 65% for 24 h. The sample thickness was measured by screw micrometer before mechanical measurement. The tensile strength at break, elongation at break, and Young's modulus of the film were tested by BOSE ELF3220 testing machine (BOSE, USA). The clamping distance and tensile speed were 20 mm and 2 mm·min^{-1}, respectively, and each sample measurement was repeated six times.

2.3.3 LED lamp bead test and flexible display

The SF/PEDOT film was placed in a room with a constant temperature of 20°C and RH of 65% for 24 h, and a simple circuit composed of 3 W light-emitting diode (LED) beads, SF/PEDOT film, SZT-C rapid constant voltage tester (Suzhou Lattice Electronics Co., Ltd.), and wires was assembled. Once the power switch was turned on, the small bulb started to light. The change in the brightness of the small bulb was observed and the circuit current value was recorded. The conductivity of SF/PEDOT film samples was tested by ST-2258C multi-function digital four-probe tester (Suzhou Lattice Electronics Co., Ltd., China), and five points for each film were tested to calculate the average value and variance.

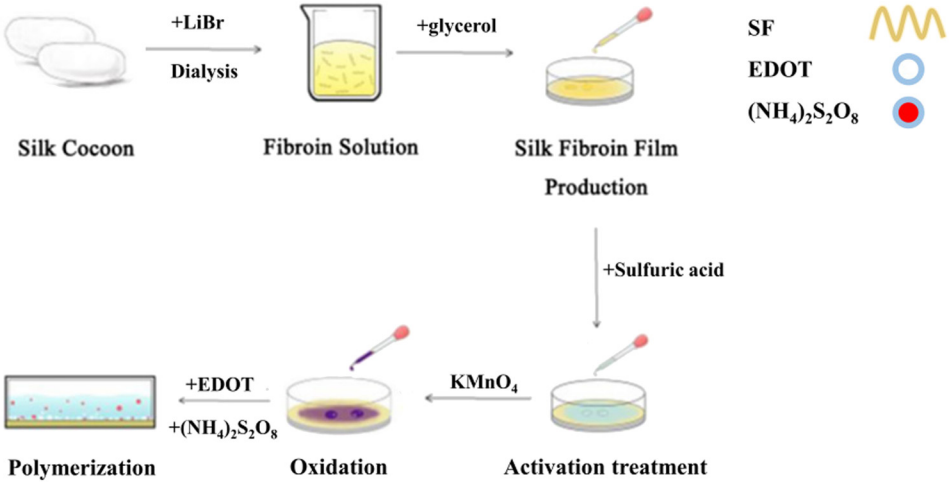

Figure 2: Flow chart for preparation of SF/PEDOT film.

2.3.4 The abrasion resistance

The abrasion resistance of the modified membranes was tested using a Martindale abrasion tester (YG401G, Ningbo Textile Instruments Co., Ltd., China). The test procedure was carried out in a standard atmosphere (20°C and RH of 65%) with a load of 9 kPa on the film. The bonding of PEDOT to the SF film was investigated by the dissolution of PEDOT in *N*-methyl-pyrrolidone (NMP). The SF/PEDOT membrane was immersed in the NMP solution at 30°C for 24 h and the color change in the solution was observed. The adhesion fastness of the membrane was investigated by observing the surface changes before and after the adhesion of the transparent adhesive tape.

2.3.5 Biocompatibility

The MTT assay was used to detect the cell activity, thus providing a proof of the biocompatibility of the conductive SF/PEDOT membrane. The pure SF film and conductive SF/PEDOT membrane were soaked in 2 mL of DMEM complete medium for 48 h, and the supernatant was taken as the sample leachate. In a sterile environment, the L929 cells were cultured in minimum essential medium containing 10% fetal bovine serum in a 5% CO_2 incubator at 37°C. The cells were digested with trypsin to prepare a single cell suspension, which was centrifuged (1,000 g, 5 min), and the cells were re-dispersed in the culture medium. The cell density was adjusted to $1 \times 10^5\ mL^{-1}$ cell suspension and was inoculated into 96-well culture plate (100 µL/well), and cultured in a 5% CO_2 incubator at 37°C. After 24 h, the original culture medium was discarded and the sample leachates were diluted with culture medium to the concentrations of 100%, 75%, 50%, and 25%, and blank control were added and continued to culture for 24 h. Then, the culture plate was taken out to observe the cell morphology. The culture medium was discarded, and $1\ mg{\cdot}mL^{-1}$ 3-(4,5-dimethylthiazol-2)-2,5-diphenyltetrazole bromide (MTT) (50 µL/well) was added and the supernatant was discarded after 4 h of incubation. 100 µL of isopropanol was added to each well to dissolve the crystals, and the microplate was shaken with a microplate shaker and the absorbance values were measured with a Synergy HT microplate reader (BIO-TEK, USA). The data were averaged, and the standard deviation was calculated as follows:

$$\text{Cell survival rate (\%)} = \frac{[OD_{570}] \text{ of the test sample group} - [OD_{570}] \text{ of the blank control group}}{[OD_{570}] \text{ of the control group} - [OD_{570}] \text{ of the blank control group}} \quad (1)$$

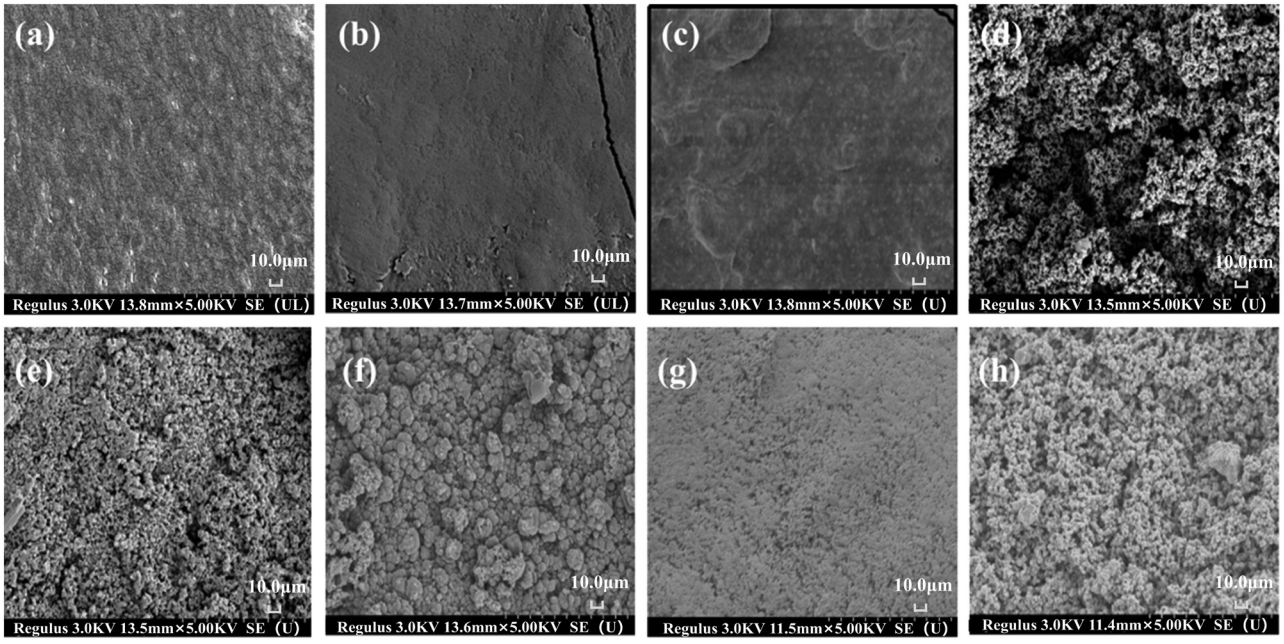

Figure 3: SEM image of (a) pure SF and (h) pure PEDOT. (b–g) The surface morphology of SF/PEDOT membranes prepared at 0.5, 1, 2, 4, 8, and 16 h, respectively.

The results were used to determine cytotoxicity according to ISO 10993-5:2009.

3 Results and discussion

3.1 Surface morphology and chemical composition analysis

Figure 3a is the SEM image of pure SF film without any treatment, and its surface is smooth. Figure 3b–g show the surface morphology of SF film after 0.5, 1, 2, 4, 8, and 16 h reaction in PEDOT solution, respectively. Due to the slow polymerization rate of EDOT, the surface morphology of SF membrane did not change significantly. When the reaction time was from 0.5 to 1 h, obvious granular PEDOT was formed on the surface of the SF film at 2–4 h; however, the distribution of PEDOT was not uniform. The surface of the SF film was covered with dense PEDOT layer at 8–16 h, and the distribution was more uniform and the PEDOT particles were more complete. Figure 3h shows the polymer morphology observed after drying the PEDOT solution after 8 h of reaction. The surface morphology is consistent with the surface morphology of SF/PEDOT membrane prepared after 8 h of polymerization (Figure 3f). SEM results show that the amount of grafted polymer on the surface of the SF membrane has a great relationship with reaction time. With the increase in the polymerization time, the amount of PEDOT grafted on the surface of the SF membrane increases and becomes more uniform.

3.2 Chemical structure

Figure 4a is the XPS high resolution Mn2p spectrum of the oxidized SF film. The two characteristic peaks correspond to the electrons of Mn at $2p_{1/2}$ (653.95 eV) and $2p_{3/2}$ (642.45 eV) (20–22), which are in general agreement with the standard value of MnO_2 (641.7 eV), demonstrating that the main existing form of Mn in the sample is +4 valence. MnO_2 was formed after the SF film was oxidized by potassium permanganate, which was stable on the surface of the SF film due to the formation of coordination with oxygen atoms on the surface of the SF film. It provided oxidation conditions for the subsequent reaction process, so that EDOT can be oxidized and grafted onto the surface of the SF film. Figure 4b shows the FTIR spectra of pure SF film and SF/PEDOT membrane reacted for 8 h. The peaks at 1,630 and 1,518 cm^{-1} are characteristic peaks of amide I and amide II of SF. The vibration peak originated from C=C on the aromatic ring of PEDOT appears at 1,443 cm^{-1} (23). The characteristic peak at 1,315 cm^{-1} is attributed to the inter-cyclic stretching of the C–C mode (24), and the peaks at 1,178 and 1,048 cm^{-1} are assigned to the bending vibration of C–O–C in ethylene dioxy (25). The absorption peaks at 972 and 834 cm^{-1} are characteristic peaks of stretching vibration of C–S–C bond in thiophene ring (20). Figure 4c shows the Raman spectra of pure polythiophene and conductive SF membrane with reaction time of 8 h. The peaks at 434, 698, 991, and 1,256 cm^{-1} correspond to C–O–C deformation, symmetric C–S–C deformation, oxyethylene ring deformation, and Cα–Cα inter-ring stretching, respectively. The characteristic peak at 1,425 cm^{-1} indicates high level of conjugation in PEDOT structure (26,27). FTIR and Raman results confirm

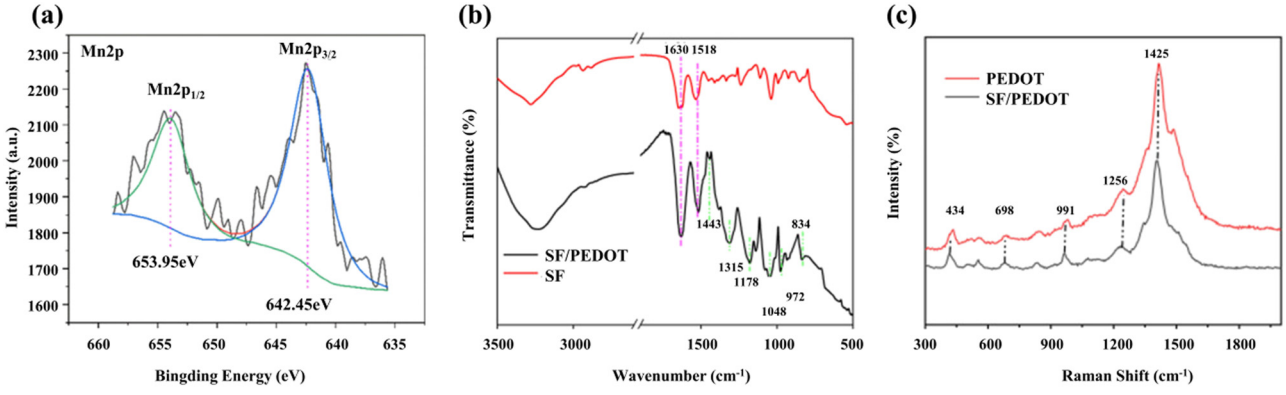

Figure 4: (a) The XPS high resolution Mn2p spectrum of oxidized SF film. (b) FTIR spectra of SF and SF/PEDOT membrane. (c) Raman spectra of pure PEDOT reacted for 8 h and SF/PEDOT membrane reacted for 8 h.

Table 1: Surface elemental compositions of SF/PEDOT membrane prepared at different time

Atomic (%)	Sample							
	Pure SF	0 h	0.5 h	1 h	2 h	4 h	8 h	16 h
C	61.17	40.22	63.33	66.72	64.98	68.01	66.81	67.35
N	9.87	5.01	7.52	3.24	3.72	1.66	5.06	3.10
O	28.93	40.51	22.69	23.82	23.62	21.45	19.02	20.69
S	0.03	0.16	4.89	5.22	7.54	8.86	9.11	8.86
Mn	0.00	14.10	1.97	1.00	0.14	0.02	0.00	0.00

that PEDOT was successfully grafted onto the surface of the SF films.

The chemical composition of SF film surface was determined by EDS. The surface element contents of SF/PEDOT membrane at different reaction times are listed in Table 1. The surface of pure SF film contains C, N, O, and S elements, and a small amount of S element comes from the sulfur containing amino acids of SF. After oxidation treatment, that is, when the reaction time is 0 h, $KMnO_4$ can react with phenolic hydroxyl, amino, and other reducing groups on the surface of the SF film to form nano manganese dioxide, which can form coordination with oxygen atoms on the surface of the SF film and exists stably. The surface of the SF film increases by 14.106% of Mn element. With the increase in reaction time, more and more PEDOT was grafted on the surface of the SF membrane, covering the nano manganese dioxide coordinated on the surface. The content of Mn element on the surface of the SF membrane decreased, while the content of S element increased. When the reaction time was 8 h, Mn element was completely covered, and the content of S element was up to 9.11%.

3.3 Mechanical properties, conductivity, and stability

In order to understand the performance of SF/PEDOT membrane, the effect of reaction time on breaking strength

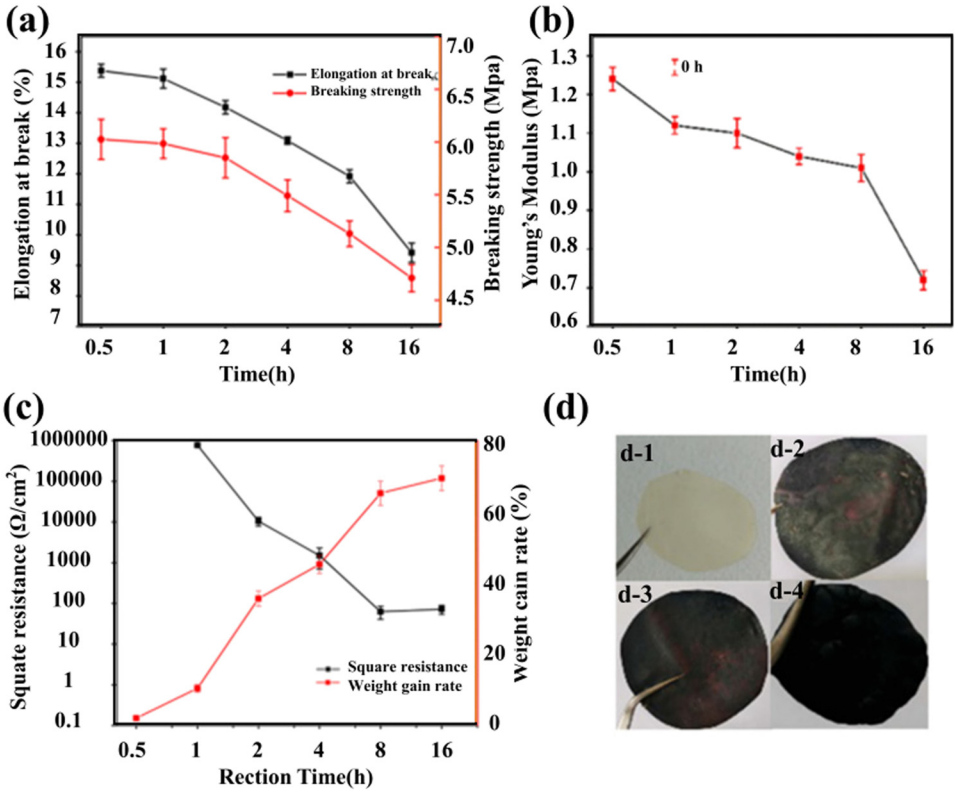

Figure 5: Mechanical properties of SF/PEDOT membrane. (a) Effect of reaction time on breaking strength and elongation at break, (b) Young's modulus, (c) square resistance and weight gain. (d) The appearance color of the SF film, Pure SF film (d-1) and SF/PEDOT membrane with reaction time of (d-2) 0 h, (d-3) 0.5 h, and (d-4) 8 h.

and breaking elongation (Figure 5a), Young's modulus (Figure 5b), and square resistance and weight gain rate (Figure 5c) were tested. As shown in Figure 5, as the reaction time increases, the mechanical properties gradually decrease. This is due to the increase in PEDOT bonded on the surface of the SF film, which changes the original structure of the SF film. When the reaction time is 8 h, the weight gain rate of the SF film reaches 65%, the sheet resistance is the smallest (63 $\Omega \cdot cm^{-2}$), and the conductivity of the SF film is the best. Since the reaction time will cause unavoidable damage to the mechanical properties of the SF film, combined with the effect of the reaction time on the conductivity of the SF film, the polymerization time is determined as 8 h. The appearance color of the SF film is displayed in Figure 5d. The pure SF film (Figure 5d-1) is milky white, which turns brown after potassium permanganate treatment (Figure 5d-2) and becomes more and more black after reaction in PEDOT solution for 0.5 h (Figure 5d-3) and 8 h (Figure 5d-4).

In order to investigate the service stability of SF/PEDOT membrane, its washing resistance stability and abrasion resistance were tested. The stability of washing resistance was to rinse the SF/PEDOT membrane with running water for 3 min each time for 5 times, and the resistance change was tested. The results are shown in Figure 6a. The resistance of SF/PEDOT membrane before washing is about 200 $\Omega \cdot cm^{-2}$. As the number of washings increases, the resistance gradually increases. After washing for 15 min, the resistance is about 500 $\Omega \cdot cm^{-2}$. This is mainly because as the number of washings increases, a small amount of PEDOT not bonded to the SF film is removed. In general, the prepared SF/PEDOT still retains good electrical conductivity because the resistance just slightly increases under prolonged washing.

Figure 6b shows the abrasion resistance result of SF/PEDOT membrane. The resistance of SF/PEDOT membrane is 800 $\Omega \cdot cm^{-2}$ after 50 times of rubbing, and the resistance is about 7,000 $\Omega \cdot cm^{-2}$ after 100 times of rubbing. The PEDOT on the surface of the SF film will fall off with the increase in the number of abrasions, and the surface resistance becomes larger. When the number of rubbing is 400 times, the resistance reaches 65 $k\Omega \cdot cm^{-2}$, and physical rubbing has a great influence on the conductivity of SF/PEDOT membrane. In Figure 6c, the tape is clean and transparent after adhesion with SF/PEDOT membrane reacted for 8 h, and there is no PEDOT on the surface of the membrane, which proves that PEDOT forms covalent bond with the phenolic hydroxyl groups of SF film instead of simple deposition on the film surface. Figure 6d shows that although the resistance of the SF/PEDOT film increases to some extent after multiple friction, it still has conductive properties. Therefore, care should be taken to avoid high intensity of friction as much as possible during storage and use of SF/PEDOT film.

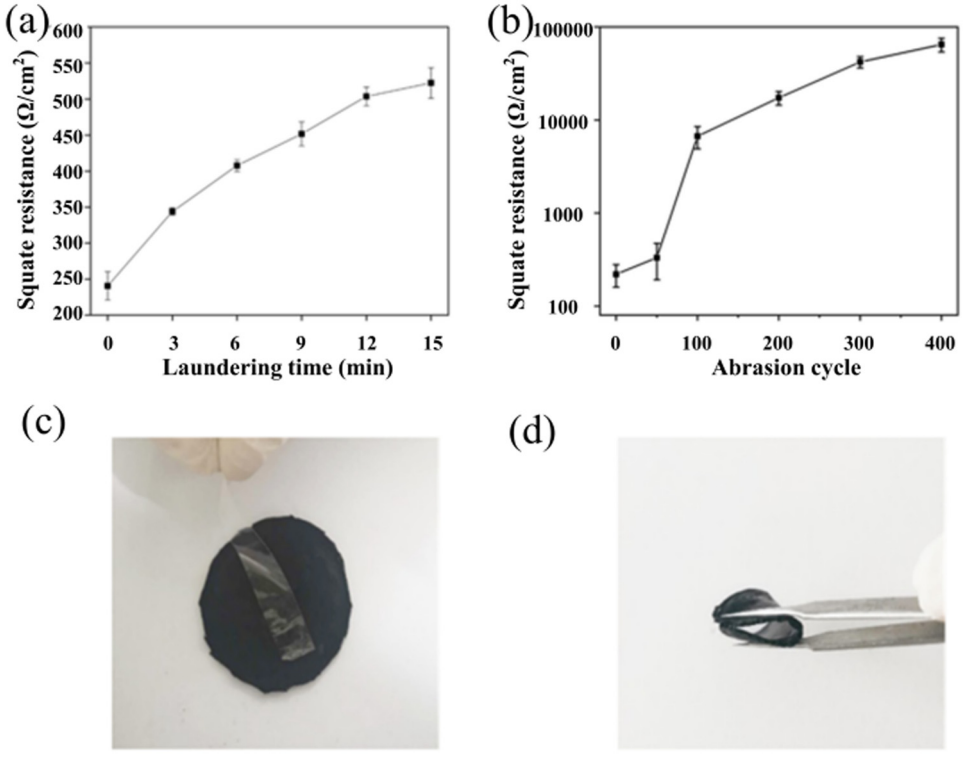

Figure 6: Effect of (a) laundering time and (b) abrasion cycles on the electrical conductivity of SF. (c) Adhesive and (d) flexible display of optimum reaction time of SF/PEDOT membrane.

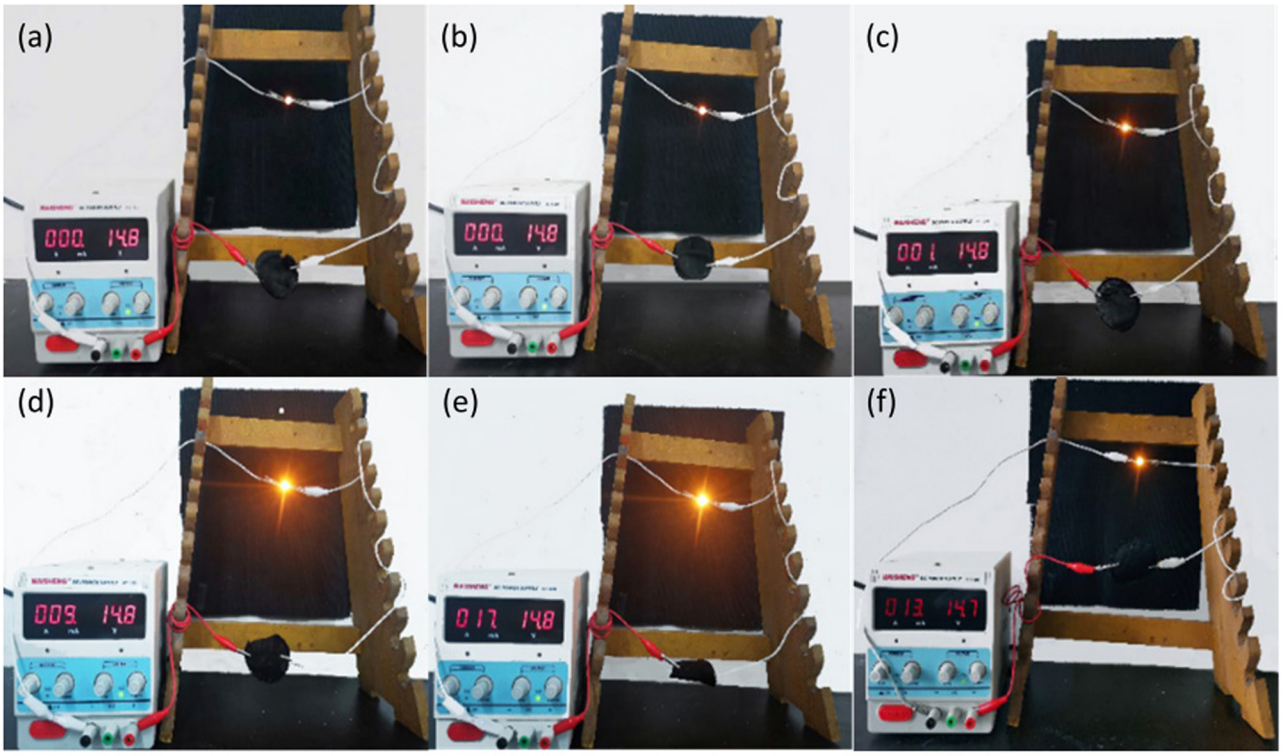

Figure 7: The LED lamp bead brightness picture of SF/PEDOT membrane prepared at different time: (a) 0.5 h, (b) 1 h, (c) 2 h, (d) 4 h, (e) 8 h, and (f) 16 h.

3.4 LED lamp bead test and flexible display

The difference in resistance can be effectively reflected by inserting SF film with different reaction time into the circuit to observe the brightness of the lamp bead and the current of the circuit as shown in Figure 7. When the reaction time is from 0.5 (Figures 7a) to 1 h (Figure 7b), the bulb has weak light, and the SF film has weak conductivity, but the current value is zero. As the reaction time increases, the PEDOT on the surface continues to increase and the conductivity of the SF film keeps increasing. When the reaction time is 8 h (Figure 7e), the current value and the brightness of the lamp bead reach the maximum.

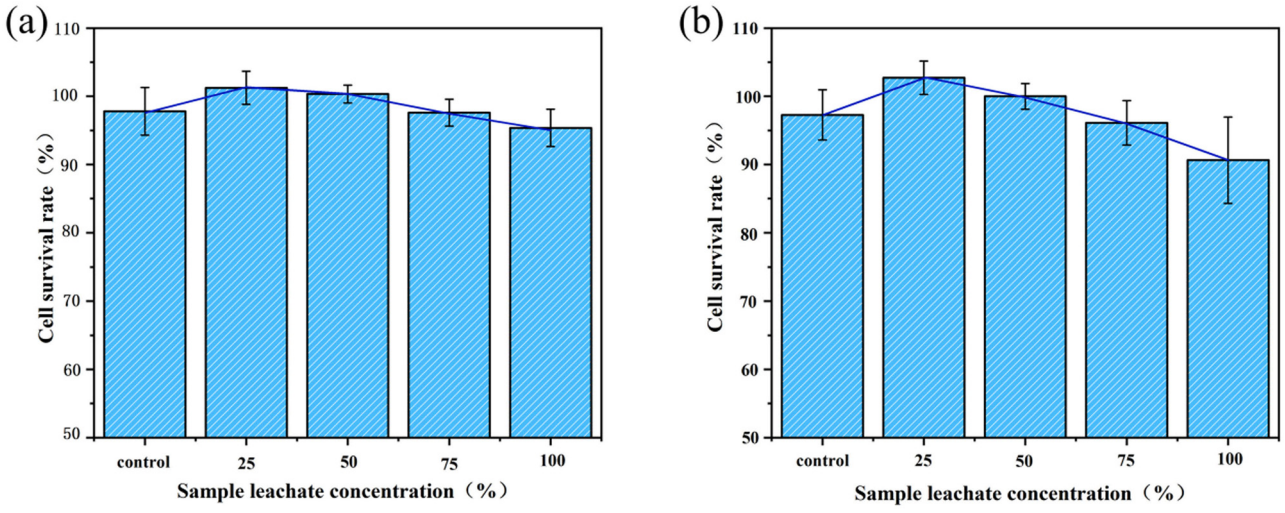

Figure 8: Cell survival rate of SF film: (a) pure SF film and (b)SF/PEDOT membrane.

3.5 Biocompatibility

The cell survival rate of different concentrations of sample leachates in pure SF film (Figure 8a) and SF/PEDOT membrane (Figure 8b) were obtained. It can be found that the cell survival rate is always greater than 70%. According to ISO 10993-5:2009, it can be concluded that the SF film (Figure 8a) and SF/PEDOT membrane both have no cytotoxicity. From the above results, the SF/PEDOT membrane has good biocompatibility, therefore it has potential applications in biomedical field.

4 Conclusion

In this work, SF/PEDOT membrane with high conductivity ($63 \pm 22\,\Omega{\cdot}cm^{-2}$) was successfully prepared by oxidative radical polymerization. The SF/PEDOT membrane has good conductivity, flexibility, and biocompatibility. FTIR and NMP dissolution results proved that PEDOT is bonded with SF film, so that SF/PEDOT membrane has good abrasion resistance and washing stability. The prepared SF/PEDOT membrane has potential applications in the fields of conductive biomaterials and flexible electronic devices.

Funding information: This work was supported by the National Natural Science Foundation of China (Grant No. 51973144 and 51741301), the Major Program of Natural Science Research of Jiangsu Higher Education Institutions of China (20KJA540002) and the Priority Academic Program Development (PAPD) of Jiangsu Higher Education Institutions for Textile Engineering in Soochow University.

Author contributions: Xin Ai contributed to results analysis, original draft, writing-review, and formal analysis; Shuqing Lu ran the experiments, tests, and results analysis; Ailing Xie performed data aggregation and graphic; Haoran Zhang assisted in experiments, tests, and data summary; Juntao Zhao carried out experiments and tests; Tianjiao Wang ran experiments; Guoqiang Chen provided technical support; Shenzhou Lu gave theoretical guidance and results analysis; Tieling Xing provided theoretical guidance, review, and editing of manuscripts.

Conflict of interest: Authors state no conflicts of interest.

Data availability statement: Data are available upon request.

References

(1) Alvi F, Ram MK, Basnayaka PA, Stefanakos E, Goswami Y, Kumar A. Graphene-poly ethylenedioxythiophene conducting polymer nano composite based supercapacitor. Electrochim Acta. 2011;56:9406–12.
(2) Islam GMN, Ali A, Collie S. Textile sensors for wearable applications: a comprehensive review. Cellulose. 2020;27:6103–31.
(3) Zhao SF, Li JH, Cao DX, Zhang GP, Li J, Li K, et al. Recent advancements in flexible and stretchable electrodes for electromechanical sensors: strategies, materials, and features. ACS Appl Mater Interfaces. 2017;9:12147–64.
(4) Naskar D, Sapru S, Ghosh AK, Reis RL, Dey T, Kundu SC. Nonmulberry silk proteins: multipurpose ingredient in biofunctional assembly. Biomed Mater. 2021;16(6):30–2.
(5) Wang QS, Zhou SQ, Wang L, You RC, Yan SQ, Zhang Q, et al. Bioactive silk fibroin scaffold with nanoarchitecture for wound healing. Compos Part B. 2021;224:109165.
(6) Guo P, Du P, Zhao P, Chen X, Liu CY, Du Y, et al. Regulating the mechanics of silk fibroin scaffolds promotes wound vascularization. Biochem Biophys Res Commun. 2021;574:78–84.
(7) Tian YK, Wu QT, Li F, Zhou YH, Huang D, Xie RJ, et al. A flexible and biocompatible bombyx mori silk fibroin/wool keratin composite scaffold with interconnective porous structure. Colloids Surf Biointerfaces. 2021;208:112080.
(8) Nguyen NT, Sarwar MS, Preston C, Goff AL, Plesse C, Vidal F, et al. Transparent stretchable capacitive touch sensor grid using ionic liquid electrodes. Extrem Mech Lett. 2019;33:100–574.
(9) Malhotra U, Maity S, Chatterjee A. Polypyrrole-silk electroconductive composite fabric by in situ chemical polymerization. J Appl Polym Sci. 2015;132:1–10.
(10) Tseghai GB, Mengistie DA, Malengier B, Fante KA, Langenhove LV. PEDOT:PSS-based conductive textiles and their applications. Sensors. 2020;20:1–18.
(11) Chen CY, Huang SY, Wan HY, Chen YT, Yu SK, Wu HC, et al. Electrospun hydrophobic polyaniline/silk fibroin electrochromic nanofibers with low electrical resistance. Polymers. 2020;2102:2–12.
(12) Erkmen C, Kurbanoglu S, Uslu B. Fabrication of poly(3,4-ethylenedioxythiophene)-iridium oxide nanocomposite based tyrosinase biosensor for the dual detection of catechol and azinphos methyl. Sens Actuators B Chem. 2020;316:121–8.
(13) Ashraf A, Farooq U, Farooqi AB, Ayub K. Electronic structure of polythiophene gas sensors for chlorinated analytes. J Mol Model. 2020;26:2–17.
(14) Hür E, Varol GA, Arslan A. The study of polythiophene, poly(3-methylthiophene) and poly(3,4-ethylenedioxythiophene) on pencil graphite electrode as an electrode active material for supercapacitor applications. Synth Met. 2013;184:16–22.
(15) Xia Y, Lu Y. Fabrication and properties of conductive conjugated polymers/silk fibroin composite fibers. Compos Sci Technol. 2008;68:1471–9.
(16) Wang XP, Meng S, Ma WJ, Pionteck J, Gnanaseelan M, Zhou Z, et al. Fabrication and gas sensing behavior of poly(3,4-ethylenedioxythiophene) coated polypropylene fiber with engineered interface. React Funct Polym. 2017;11:2–5.

(17) Im SG, Olivetti EA, Gleason KK. Systematic control of the electrical conductivity of poly (3,4-ethylenedioxythiophene) via oxidative chemical vapor deposition. Surf Coat Technol. 2007;201:9406–12.
(18) Lu G, Li C, Shi G. Synthesis and characterization of 3D dendritic gold nanostructures and their use as substrates for surface-enhanced Raman scattering. Chem Mater. 2007;19:3433–40.
(19) Liu BC, Zhao Y, Cai X, Xie Y, Wang YT, Cheng DL, et al. A wireless, implantable optoelectrochemical probe for optogenetic stimulation and dopamine detection. Microsyst Nanoeng. 2020;6:2–12.
(20) Niu PF, Cai YC, Guo M, Shen ZL, Li MC. Preparation and electrochemical performance of TEMPO-modified polyterthiophene electrode obtained by electropolymerization. Electrochem Commun. 2020;110:106623.
(21) Chacón-Patiño ML, Blanco-Tirado C, Hinestroza JP, Combariza MY. Biocomposite of nanostructured MnO2 and fique fibers for efficient dye degradation. Green Chem. 2013;15:2920–8.
(22) Huang S, Wang L, Liu L, Hou Y, Li L. Nanotechnology in agriculture, livestock, and aquaculture in China: a review. Agron Sustain Dev. 2015;35:369–400.
(23) Cheng YH, Kung CW, Chou LY, Vittal R, Ho KC. Poly(3,4-ethylenedioxythiophene) (PEDOT) hollow microflowers and their application for nitrite sensing. Sens Actuators B Chem. 2014;192:762–8.
(24) Ely F, Matsumoto A, Zoetebier B, Peressinotto VS, Hirata MK, Sousa DA, et al. Handheld and automated ultrasonic spray deposition of conductive PEDOT:PSS films and their application in ACEL devices. Org Electron. 2014;15:1062–70.
(25) Wang H, Yue L, Wang XW. Imitation-mussel-based high-performance conductive coating on hydrophobic fabric for thermochromic application. J Appl Polym Sci. 2019;136:1–6.
(26) Tamburri E, Orlanducci S, Toschi F, Terranova ML, Passeri D. Growth mechanisms, morphology, and electroactivity of PEDOT layers produced by electrochemical routes in aqueous medium. Synth Met. 2009;159:406–14.
(27) Wu D, Zhang J, Dong WL, Chen HW, Huang X, Sun BQ, et al. Temperature dependent conductivity of vapor-phase polymerized PEDOT films. Synth Met. 2013;176:86–91.